

REPORT DOCUMENTATION PAGE

Form Approved
OMB No. 074-0188

Public reporting burden for this collection of information is estimated to average 1 hour per response, including the time for reviewing instructions, searching existing data sources, gathering and maintaining the data needed, and completing and reviewing this collection of information. Send comments regarding this burden estimate or any other aspect of this collection of information, including suggestions for reducing this burden to Washington Headquarters Services, Directorate for Information Operations and Reports, 1215 Jefferson Davis Highway, Suite 1204, Arlington, VA 22202-4302, and to the Office of Management and Budget, Paperwork Reduction Project (0704-0188), Washington, DC 20503

1. AGENCY USE ONLY (Leave blank)	2. REPORT DATE June 15 th , 2006	3. REPORT TYPE AND DATES COVERED Final Report: 09/15/2004-06/14/2006
---	---	--

4. TITLE AND SUBTITLE High Power Mid Wave Infrared Semiconductor Lasers	5. FUNDING NUMBERS Award Number <i>F49620-03-1-0437</i> Total Amount: \$302,122.00
---	---

6. AUTHOR(S)
Sanjay Krishna, Assistant Professor University of New Mexico
Ralph Dawson, Research Professor, University of New Mexico

7. PERFORMING ORGANIZATION NAME(S) AND ADDRESS(ES)
Technical Point of Contact
Prof. Sanjay Krishna,
1313 Goddard SE, Albuquerque NM
Phone: 505 2727892, Fax 505 272 7 801

8. PERFORMING ORGANIZATION REPORT NUMBER
Final Progress Report

9. SPONSORING / MONITORING AGENCY NAME(S) AND ADDRESS(ES)

USAF, AFRL AFOSR/NE 4015 Wilson Blvd, Rm 713 Arlington VA 22203-1954 Kathryn Pheulpin 70 696 9735	Missile Defense Agency, Dr. Pravat K. Choudhury, RM # Annex G-805A7100 Defense Pentagon, Washington, DC 20301-7100 (703)-697-8012, Fax (703) 695-6582
---	---

10. SPONSORING / MONITORING AGENCY REPORT NUMBER
Final Progress Report

11. SUPPLEMENTARY NOTES
Technical Monitor: Dr. Donald Silversmith, AFOSR/NE 703 588-1780

AFRL-SR-AR-TR-07-0068

12a. DISTRIBUTION / AVAILABILITY STATEMENT
Copies sent to MDA, AFOSR and ONR
Distribution Statement A: unlimited

13. ABSTRACT (Maximum 200 Words)
This project identifies key challenges for the development of high-power electrically injected MWIR laser arrays using III-V antimonide based materials. In this approach, InGaSb quantum wells are grown on metamorphic layers on a GaSb or GaAs substrate. Doping of these layers is extremely challenging. We have obtained activation energies for Te-doped and Be-doped InAlSb. Using a novel interlayer doping schemes, we have been able to fabricate high quality PIN diodes. We have also filed a provisional patent on semiconductor conducting layers. The license for this patent is presently being negotiated by the University tech transfer office with a small business firm in new mexico. We have also demonstrated room temperature photoluminescence up to 3 μm from InGaSb quantum wells grown on GaAs substrate. Using this approach we have fabricated optically pumped vertical cavity surface emitting lasers.

14. SUBJECT TERMS: Mid infrared, semiconductor lasers, doping, metamorphic

15. NUMBER OF PAGES
4
16. PRICE CODE

17. SECURITY CLASSIFICATION OF REPORT
Unclassified

18. SECURITY CLASSIFICATION OF THIS PAGE
Unclassified

19. SECURITY CLASSIFICATION OF ABSTRACT
Unclassified

20. LIMITATION OF ABSTRACT
None

FINAL REPORT FOR AWARD NUMBER F49620-03-1-0437

Technical Progress Description

Development of Electrically Injected Devices

In recent years, there has been considerable interest in the development of mid-wavelength infrared (MWIR) emitters operating in the spectrum approximately between 2 and 5 μm ¹⁻⁶. Applications for devices operating in this region include remote sensing of trace gases (gas spectroscopy), Laser Detection and ranging (LADAR), surveillance and reconnaissance, missile tracking and infrared countermeasures, free-space communication, polymer etching, and blood glucose level monitoring. Advances in epitaxial growth of semiconductor materials have allowed the development of Arsenic-free optically-pumped MWIR lasers on GaSb substrates using relaxed, step graded metamorphic $\text{In}_x\text{Al}_{1-x}\text{Sb}$ buffer layers grown using a digital-alloyed strained layer superlattice filtering technique. Room temperature (RT) quasi continuous-wave (CW) optically pumped edge-emitting lasers have been realized, operating at wavelengths between 2.5 and 3.3 μm , with the best devices producing output powers in excess of 0.4W/facet, characteristic temperatures up to $T_0=119\text{K}$, and differential quantum efficiencies as high as $\eta_d=28\%$ ¹. By comparison, GaSb lattice-matched lasers utilizing InGaAsSb/AlGaAsSb active regions and operating CW at similar wavelengths have lower characteristic temperatures (T_0) of between 31K and 62K²⁻⁴. The higher value of T_0 for As-free materials is attributed to improved confinement for both electrons and holes due to the inherent type-I band-edge alignment and the larger valence band in this material system. However, to date no electrical operation of these mid-IR type-I

Arsenic-free lasers has been reported. Doped laser structures exhibited resistivities too high to be useful as a diode, and the free carrier concentrations within the $\text{In}_x\text{Al}_{1-x}\text{Sb}$ buffer layers were much lower than expected, regardless of efforts to more heavily dope the metamorphic buffer structure⁷.

To understand the poor electrical performance of the buffer layers and to further optimize the doping so as to realize electrically pumped laser structures, the doping behavior in the $\text{In}_x\text{Al}_{1-x}\text{Sb}$ layers must be better understood. Therefore, in this project, we have undertaken a detailed study of the Be and Te doping of $\text{In}_x\text{Al}_{1-x}\text{Sb}$. To the best of our knowledge this is the first report of activation energies in this material system and will provide invaluable information for realizing electronic and optoelectronic devices based on this system.

Antimonide materials appear to be less easily doped than Arsenides and this is especially true for n-type doping. The most common donor in GaAs, Silicon, is more amphoteric in GaSb and practically a good acceptor in AlSb⁸. Instead the majority of this study was performed on n-type materials with Tellurium as the n-type dopant and Be as the p-type dopant. The activation energy of Beryllium in $\text{In}_x\text{Al}_{1-x}\text{Sb}$ is low, and the achievable ionized carrier concentration levels are comparable to GaAs ($>10^{18}\text{cm}^{-3}$ p-type). Three different compositions of $\text{In}_x\text{Al}_{1-x}\text{Sb}$ were doped with Beryllium to verify the inherent low activation energy.

N-type and P-type AlSb, and various compositions of $\text{In}_x\text{Al}_{1-x}\text{Sb}$, were grown by solid-source molecular beam epitaxy on semi-insulating GaAs substrates, the substrate chosen due to the unavailability of an insulating GaSb substrate. Thick (3 to 13 μm), relaxed (metamorphic) layers of $\text{In}_x\text{Al}_{1-x}\text{Sb}$ were deposited at growth rates between 0.4

and 1.0 $\mu\text{m/hr}$. All samples were grown between 470°C and 515°C as measured by a 1.0- μm pyrometer, with the lower growth temperatures reserved for samples containing a higher Indium fraction. The GaTe source was fixed at either 475°C or 500°C for all of the growths, providing a Te incorporation between approximately $5 \times 10^{17} \text{cm}^{-3}$ and $1 \times 10^{18} \text{cm}^{-3}$, and the Be source was fixed at 820°C. The V/III ratio was kept between 3:1 and 5:1. The dopant source shutter was opened after the characteristic 1X3 RHEED pattern was observed. After growth, samples were cleaved into 10mm by 10mm squares and Indium contacts sintered onto each corner at $\sim 160^\circ\text{C}$ for 5 minutes. Ionized carrier densities were measured using the Van der Pauw/Hall technique between 300 K and 380 K. Room-temperature carrier densities between mid- 10^{15}cm^{-3} and low- 10^{18}cm^{-3} were obtained. A range in ionized carrier concentration was observed and could be a result of a number of factors including relative dopant cell position on the source flange, dopant cell temperature, growth temperature, growth rate, V:III ratio, and most importantly activation energy of the dopant element within the particular composition of interest. The temperature dependent concentration data for each composition were formed into an Arrhenius plot ($\ln N$ vs. $1/kT$), and the activation energy (E_A) of the dopant was extracted from the characteristic linear slope. Symmetric (004) and asymmetric (115) X-ray diffraction scans were performed on all the grown samples to confirm the compositions using the epitaxial layer and substrate peak separation.

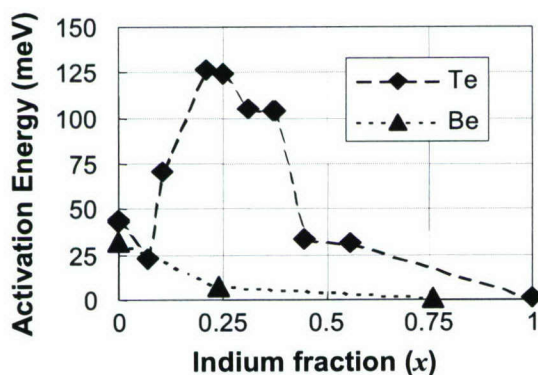


Figure 1: Compositional dependence of Beryllium acceptor activation energy and Tellurium donor activation energy in $\text{In}_x\text{Al}_{1-x}\text{Sb}$.

Results indicate that Beryllium in AlSb forms an acceptor level 32 meV above the valence band edge and becomes more shallow as the Indium content is increased, as shown in Fig. 1. Tellurium in AlSb forms a donor level 43-44 meV below the conduction band (CB) edge. However for Tellurium in $\text{In}_x\text{Al}_{1-x}\text{Sb}$, the donor level is a very strong function of composition, with measured values ranging between 22meV and 126meV below the CB edge, also shown in Fig. 1. A literature value for the Te donor level for InSb is also indicated⁹. Over the range of Indium composition $0.1 < x < 0.4$, the donor atoms appear to form a very deep level below the conduction band. In this composition range, based on the measured E_A , approximately 1% of incorporated carriers become ionized to contribute to conduction. This result is consistent with the measured carrier concentration (two orders of magnitude lower) in the $\text{In}_x\text{Al}_{1-x}\text{Sb}$ ternary versus an equivalently incorporated concentration of Te in GaAs. The results are also consistent with the high resistivities of early electrically-injected laser attempts since those laser structures were grown on either $\text{In}_{0.27}\text{Al}_{0.73}\text{Sb}$ or $\text{In}_{0.36}\text{Al}_{0.64}\text{Sb}$ metamorphic buffers⁷, i.e., layers with high E_A . It is not clear what is the cause of the deep level, however a likely explanation is donor-exiton binding (DX center)¹⁰. A similar composition-dependence of the activation energy has been observed for Si-doped AlGaAs ¹¹, where activation energies were markedly higher for alloy compositions close to the direct-indirect cross-over point, as well as in GaSb ¹², where higher than expected

activation energies are attributed to the small energy difference between the Γ and L conduction band minima.

A clear illustration of the effect of activation energy on carrier concentration is shown in Fig. 2. Plots of the logarithm of the measured carrier density, as a function of reciprocal temperature for several different compositions of $\text{In}_x\text{Al}_{1-x}\text{Sb}$ are compared. For the compositions $x=7\%$, $x=11\%$ and $x=45\%$, the carrier concentrations are higher and the characteristic slopes are shallower than for $x=21\%$ and $x=31\%$, indicating low activation energies and a relatively shallow donor for these compositions. A transition occurs between 38% and 45% Indium that causes the donors to become dominantly shallow. Our speculation as the reason for this change is the bandgap crossover from the X to the Γ valley near 40% Indium, although this crossover is not very well documented for this material system.

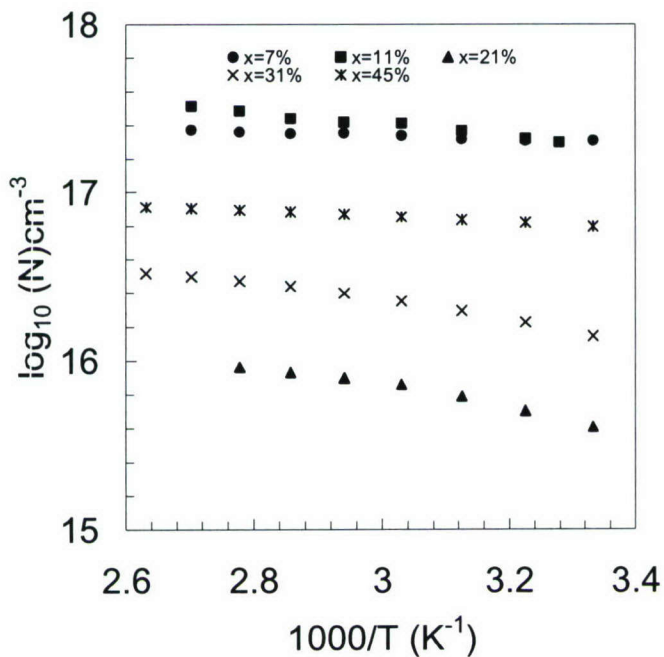


Figure 2: Carrier concentration as function of temperature for several compositions of Te-doped $\text{In}_x\text{Al}_{1-x}\text{Sb}$

To develop a highly conducting n-type clad layer, we have proposed the use of a digital alloy using constituent layers of compositions with low activation energy. For example, we propose that $\text{In}_x\text{Al}_{1-x}\text{Sb}$ with an average composition in the approximate range $0.1 < x < 0.4$ can be made highly n-type conductive if formed from short-period superlattice layers (approximately 20 – 80 Å thick periods) of Tellurium-doped AlSb and $\text{In}_{0.50}\text{Al}_{0.50}\text{Sb}$. Preliminary results indicate good conduction through such superlattice structures. An additional benefit of a strained layer superlattice is the ability to filter threading dislocations while growing mismatched with respect to the substrate. Mismatched growth is necessary using this material system since no naturally lattice-matched substrate is available.

Using the results from the composition dependent doping study, we have fabricated a PIN junction diode using materials outside of the deep-donor range of $\text{In}_x\text{Al}_{1-x}\text{Sb}$ to verify good conductivity. The diode consisted of doped $\text{In}_{0.50}\text{Al}_{0.50}\text{Sb}/\text{AlSb}$ cladding layers, with an average composition stepped from AlSb to $\text{In}_{0.4}\text{Al}_{0.6}\text{Sb}$, either side of a 1 μm thick undoped $\text{In}_{0.53}\text{Ga}_{0.21}\text{Al}_{0.26}\text{Sb}$ region. The Tellurium doping concentration within the $\text{In}_{0.50}\text{Al}_{0.50}\text{Sb}/\text{AlSb}$ lower clad was approximately $2 \times 10^{18} \text{ cm}^{-3}$ n-type. The activation energy of similar superlattices, grown on GaAs, was measured to be 32 meV. Room temperature current-voltage measurements on this sample, shown in Fig. 3, were performed on test device areas with Indium contacts measuring approximately 2mm by 2mm. The samples exhibited a turn-on voltage of ~0.4V, and a forward-biased differential resistance of 0.64Ω, the majority of which was attributed to system wiring resistance. Reverse leakage current begins to occur at 1.5V reverse

bias. By contrast, a similarly-structured and contacted early doped Arsenic-free type-I laser grown on an $\text{In}_{0.27}\text{Al}_{0.73}\text{Sb}$ metamorphic buffer on GaSb turned-on at +19V.

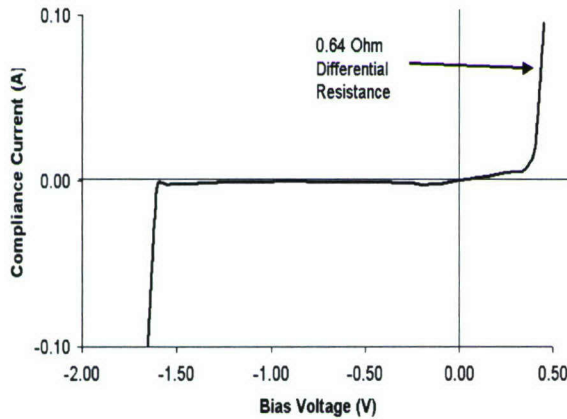


Figure 3: $\text{In}_{0.50}\text{Al}_{0.50}\text{Sb}/\text{AISb}$ PIN diode current-voltage relationship.

In conclusion, the activation energies for Be and Te in $\text{In}_x\text{Al}_{1-x}\text{Sb}$ were investigated. Whereas the activation energy for Be is <32 meV for all compositions investigated, Te is only incorporated as a relatively shallow donor for compositions with approximately $x < 0.1$ and $x > 0.45$. Using this knowledge, it should be possible to realize layers with practical doping levels for useful devices including lasers, detectors and thermophotovoltaic cells.

Development of Optically Pumped Vertical Cavity Surface Emitting Lasers

In the past few years, there has been growing interest in the development of mid infrared lasers for a variety of military and civilian applications. Semiconductor lasers are particularly attractive for applications such as infrared counter measures (IRCM) and laser detection and ranging (LADAR) because they allow the laser and infrared focal plane array to share a common aperture and enable modulation for FM LADAR applications. For spectroscopic applications such as trace-gas sensing, remote pollution monitoring, medical diagnostics, and explosive detection, it is desirable to use optoelectronic devices with a narrow, and preferably tunable, spectral linewidth. The spectra of many edge-emitting lasers display mode-hops that can change with time and can degrade spectroscopic performance. While it is possible to control the longitudinal mode behavior through complex processing to form distributed feedback (DFB) lasers, a simpler solution is a vertical-cavity based laser such as a vertical-cavity surface-emitting laser (VCSEL). The advantages of VCSELS include intrinsic single-mode behavior, due to the short cavity length and a high-quality low-divergence circular output beam. The electrical and optical pumping thresholds can be lower than for edge emitters since the active area can be quite small. Additionally, it is relatively simple to form 2-dimensional arrays of devices to obtain large output powers. While most research has concentrated on the use of VCSELS in data and telecommunication applications, their spectral characteristics make them well suited to spectroscopic applications in the mid wave infrared (MWIR, 2-5 μm).

Although MWIR lasers have been developed using lead (Pb) salts, and II-VI compound semiconductors, the most promising technological advances have been

achieved using antimonide-based III-V compound semiconductor materials lattice matched to GaSb substrates. Room temperature (RT) or near-room temperature operation of laser diodes at wavelengths shorter than 3.0 μm has been achieved. Near 2 μm type-I InGaAsSb/AlGaAsSb lasers have been reported with a characteristic threshold temperature T_0 of up to 140K. By increasing the In and/or As content of the wells, longer wavelengths have been reported (2.78 μm), but the characteristic temperature falls dramatically (58K) owing to the deleterious loss in valence band offset. Low temperature operation of 4.5 μm , InAsSb/InAlAs quantum well lasers was reported with a T_0 of 26K. Thus typically, the devices require thermoelectric or even cryogenic cooling to operate at high powers and/or long wavelength, making them difficult to incorporate into compact field-test measurement systems. Furthermore, in addition to requiring two group V elements (As and Sb) in the heterostructures, the type-II band edge alignment in the InAs/(Ga,Al)Sb material system does not favor the straightforward localization of electrons and holes in the same region of space. To minimize the separation of electrons and holes, and thus increase the efficiency of recombination and photon emission, complex heterostructures have to be designed. This leads to a complicated growth process due to the limited ability to accurately control the composition of the group V elements during the growth. This is further compounded by the anion intermixing and different types of interface bonds that occur at the various interfaces in the heterostructure.

Despite the progress in edge-emitting lasers, there have been only a few reports of optically pumped MWIR VCSELs . An optically pumped II-VI (HgCdTe) structure was demonstrated, lasing at 3.06 μm , but only at very low temperatures and high pump

intensities. A lead-salt VCSEL emitting at 4.12 μm at room temperature pulsed operation was also demonstrated, but with a very high threshold pump density of $200\text{kW}/\text{cm}^2$. Antimonide-based III-V VCSELs have been demonstrated at 2.9 μm , and 2.1 μm . Although the threshold pump densities were less than $1\text{kA}/\text{cm}^2$, low T_0 values of less than 44K were obtained, preventing continuous wave (CW) operation at room temperature. If room temperature CW performance is to be achieved, it is essential that the characteristic temperature be increased, which could be achieved by improved carrier confinement. Recently, researchers at our center have developed a technique to grow "arsenic-free" lasers on GaSb substrates using a relaxed InAlSb layer grown using a digital alloying technique. Using such a graded metamorphic buffer, optically pumped room temperature edge-emitting lasers between 2.5-3.3 μm with output powers in excess of 0.4W/facet with $T_0=119\text{K}$ and $\eta_d=28\%$ have been demonstrated [18]. In comparison, GaSb lattice-matched lasers operating at a similar wavelength had characteristic temperatures of only 58K. Room temperature detectors based on this approach have also been reported. The higher value for T_0 can be attributed to improved confinement for both electrons and holes. Thus the growth of active materials on a metamorphic InAlSb buffer layer is expected to dramatically improve the temperature performance of MWIR VCSELs. In this paper, we report the growth of optically pumped VCSELs emitting at 2.3 μm using this "Arsenic Free" design with InGaSb QWs and InGaAlSb/InAlSb DBR layers with a threshold current density of 2.5 mA/cm^2 at 77K. The thickness of the cavity and QWs were optimized to achieve an overlap between the cavity resonance and the gain spectrum.

The devices were grown using solid source molecular beam epitaxy (MBE) in a V80 reactor. Two side polished, undoped GaSb substrates (100) were used for the growth. Prior to the growth, the substrate was heated to 530 °C, under Sb over pressure, for oxide desorption and a 100 nm smoothing layer GaSb was grown. Reflection High Energy Electron Diffraction (RHEED) was used to monitor the growth. A graded metamorphic buffer terminating with a $\text{Al}_{0.73}\text{In}_{0.27}\text{Sb}$ layer was then grown using a digital alloy technique that reduces threading dislocations. The metamorphic buffer consists of a 0.5 μm thick AlSb layer followed by equal thicknesses of $\text{Al}_{1-x}\text{In}_x\text{Sb}$ layers where the indium content $x = 0.09, 0.18$ and 0.27 . Each $\text{Al}_{1-x}\text{In}_x\text{Sb}$ layer is made up of 100 periods of 50 Å superlattice of AlSb and $\text{Al}_{0.73}\text{In}_{0.3}\text{Sb}$. The metamorphic buffer enables the growth of with lattice constant larger than that of GaSb, thus enabling emission at wavelengths beyond 2 μm as mentioned elsewhere. The entire device structure was grown at 475 °C, but the growth during AlSb layer was interrupted every 500 Å for a two-minute anneal at 550 °C to further reduce dislocation density. All alloys were grown about 0.6 – 0.85 $\mu\text{m}/\text{h}$ and a group VI/ group III beam equivalent pressure ratio of ~ 6 was used. The ternary constituent of the Bragg mirror was grown as a digital alloy, where as, the quaternary constituent was grown as bulk.

The VCSEL structure consists of an active region in a λ – cavity between a 15-pair Bragg mirror stack at the bottom and a 12-pair Bragg mirror stack on the top. The Bragg reflector structure consists of $\text{Al}_{0.73}\text{In}_{0.27}\text{Sb}$ / $\text{Al}_{0.25}\text{Ga}_{0.43}\text{In}_{0.32}\text{Sb}$ quarter-wave layers. The quaternary layer in the DBR was used to reduce absorption of the emission wavelength. The active region consists of three 0.5% compressively strained $\text{Ga}_{0.57}\text{In}_{0.43}\text{Sb}$ wells, each 15 nm thick, separated by 15 nm thick $\text{Al}_{0.25}\text{Ga}_{0.43}\text{In}_{0.32}\text{Sb}$

barriers at the center of the cavity. $\text{Al}_{0.25}\text{Ga}_{0.43}\text{In}_{0.32}\text{Sb}$ also forms the spacer material of the cavity. The entire device structure is lattice matched to the metamorphic $\text{Al}_{0.27}\text{In}_{0.73}\text{Sb}$.

Before the growth of the entire VCSEL structure, the active region and the DBR layers were independently optimized. As the refractive indices of these alloy compositions were not known accurately, we used the single effective oscillator model proposed by Wemple and DiDomenico, the parametric equations proposed by Takagi, and antimonide material parameters to obtain baseline refractive indices. These parameters were integrated into a model that we developed to predict the reflectivity spectrum of the Bragg mirrors, based on the transfer matrix theory of multi-layer films. These values were used as baseline refractive indices, initially, to predict the quarter-wave thicknesses of the Bragg mirror constituent layers. The refractive index contrast between the two constituent layers is about 0.26. A few DBR calibration samples, with 7 pair top and bottom mirror stacks on either side of a λ – cavity, were then grown and characterized. SEM images were used to ascertain the thicknesses of the various layers. One such SEM image (Fig. 4) indicated good interfaces even after the growth of thick layers. The room-temperature reflectivity spectra of all samples were measured using a low power infrared white-light source to illuminate the sample and a Fourier Transform Infrared Spectrometer (FTIR) to collect and process the reflected light. Our initial samples revealed that the measured reflectivity spectra were blue shifted compared to design wavelengths, requiring an empirical correction to account for model inaccuracies are made. Figure shows the measured and calculated reflectivity spectrum of the calibration sample. Also shown in the figure is the photoluminescence

from a three stack InGaSb QWs that constitutes the active region of the VCSEL. We can see that there is a very good agreement between the dip in the cavity resonance and the peak of gain spectrum (represented by the PL, Fig 5).

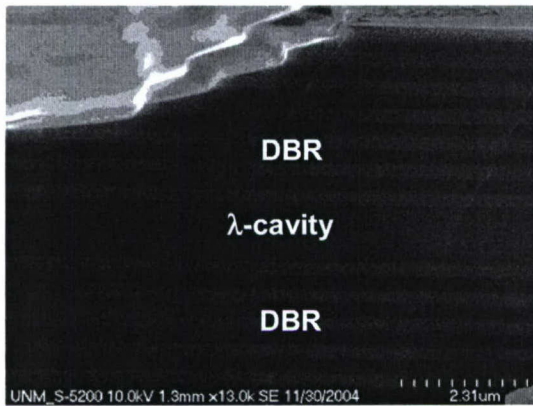


Figure 4: A scanning electron microscopy (SEM) image depicting a section of the distributed Bragg reflectors (DBR) and cavity.

After this optimization, the entire VCSEL structure was grown and optically pumped by a Topaz optical parametric oscillator (OPO) emitting at 1.4 μm . The OPO was pumped by a 1KHz Clark -MXR Ti-sapphire regenerative amplifier. Figure 6(a) shows the emission spectra of the device at 77K. The solid line shows the surface emission and the dotted line shows the emission from a cleaved edge at same excitation conditions. The edge emission spectrum, which represents spontaneous emission from the QWs, is red shifted by about 30 nm in comparison with the surface emission, which includes the effect of the cavity resonance. Figure 6(b) shows the dependence of the surface emission on the pump intensity. The figure shows two different excitation power dependencies: below an excitation intensity of 2.5mW/cm² per pulse, the intensity from the VCSELs increases only weakly with increasing pump intensity, where as, above 2.5mW/cm² per pulse, there is a steep rise of the output power for increasing optical excitation. This indicates an extremely low laser threshold of about 2.5mW/cm² per pulse. Future efforts include developing intracavity contacts to demonstrate electrically injected VCSELs.

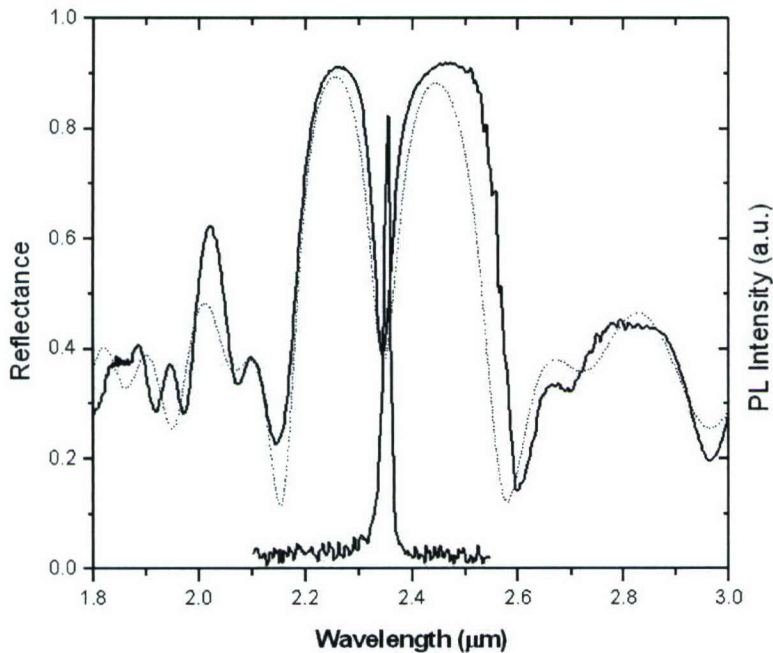


Figure 5: Calculated and measured reflectivity spectrum from a InAlSb I-cavity with 7 periods of $\text{Al}_{0.73}\text{In}_{0.27}\text{Sb}$ / $\text{Al}_{0.25}\text{Ga}_{0.43}\text{In}_{0.32}\text{Sb}$ (DBR). Also shown is the PL emission from three 0.5% compressively strained $\text{In}_{0.43}\text{Ga}_{0.57}\text{Sb}$ quantum wells. Note that there is very good agreement between the cavity resonance (dip in the reflectivity spectrum) and the gain spectrum (PL emission).

In conclusion, we report the growth, fabrication and characterization of optically pumped VCSELs emitting at 2.3 microns using an “Arsenic free” design with Type-I InGaSb QWs and InAlSb/InGaAlSb DBR. The active region and the DBRs were independently optimized to obtain an overlap between the cavity resonance and gain spectrum. Using this approach, extremely low threshold lasers, ($P_{\text{th}}=2.5\text{mW}/\text{cm}^2$) have been reported.

Names of Students Working on the Project:

- Peter Hill (Masters by Thesis, Working with Intel Corporated)
 - Ravi Kalyanam (Pursuing his PhD)
- (It is to be noted that both these students are partially funded by this project and funds from the PI’s other grants is used to supplement their support).

Names of Senior Personnel Working on the Project:

- Prof. Sanjay Krishna (PI)

- Prof. Ralph Dawson (Co-PI)
- Dr. Philip Dowd (Post doctoral associates)

(It is to be noted that the senior personnel are partially funded by this project and funds from the PI's other grants is used to supplement their support).

Publications/Presentations and Patents:

- P. Hill, N. Weisse-Bernstein, L. R. Dawson, P. Dowd, and S. Krishna, "Activation energies for Te and Be in metamorphically grown AlSb and In_xAl_{1-x}Sb layers", Appl. Phys. Lett. **87**, 092105 (2005)
- P.Hill, P. Dowd, L.R. Dawson and S. Krishna, " Optically Pumped Mid Infrared Lasers on Metamorphic Buffer Layers Grown on GaAs Substrates", Electronic Materials Conference, June 2005.
- P.Hill, P. Dowd, L.R. Dawson and S. Krishna, " Doping studies in Metamorphic AlSb and InAlSb Films", Electronic Materials Conference, June 2004
- P. Dowd, P. Hill, L.R. Dawson and S. Krishna, "Semiconductor Conductive Layers", Provisional Patent Filed with USPTO, June 2004 (Docket number 1863.047PRV)
- R. Kalyanam, L.R. Dawson and S. Krishna " Mid infrared Vertical Cavity Surface Emitting Lasers", Electronic Materials Conference, June 2006.